Numerical Simulation of Internal Plasma in a Miniature Microwave Discharge Ion Thruster

IEPC-2007-190

Presented at the 30th International Electric Propulsion Conference, Florence, Italy
September 17-20, 2007

Takayasu KANAGAWA*, Naoji YAMAMOTO†, Yoshihiro KAJIMURA‡, Hideki NAKASHIMA¶
Department of Advanced Energy Engineering Science,
Graduate school of Engineering Science,Kyushu University
6-1 Kasuga-koen, Kasuga, Fukuoka 816-8580, JAPAN

and

Hirokazu MASUI§
Department of Electrical Engineering Kyushu Institute of Technology
1-1 Sensui, Tobata, Kitakyushu, Fukuoka, 804-8550, JAPAN

Abstract: The effect of magnetic field configuration on thrust performance in a miniature microwave discharge ion thruster is investigated with numerical simulation in order to improve its thrust performance. First, an electron trajectory, and the time variations of the electron energy and the magnetic field intensity which an electron feels are calculated. The electron is heated at electron cyclotron resonance (ECR) layer, and the incremental electron energy through the ECR layer is distributed from -10 eV to 30 eV, the average being approximately 3.8 eV. The incremental energy is decreased with increase in the number of magnets, that is, with increase in the distance between the antenna and the ECR layer. Then, spatial distributions of the energy are calculated along with electron energy distribution function (EEDF) for various magnetic field strengths. With increasing the number of magnets, the high electron energy zone and the number of electrons with energy higher than the ionization potential are decreased. These would be due to the enlargement of distance between the antenna and ECR layer.

Nomenclature

m	=	mass
$\boldsymbol{v}$	=	velocity
q	=	charge of the particle
$\boldsymbol{H}$	=	magnetic field
$\boldsymbol{E}$	=	electric field
$\boldsymbol{J}$	=	current density
$\boldsymbol{B}$	=	external magnetic field
ε_0	=	permittivity
μ_0	=	permeability

*Graduated student, Department of Advanced Energy Engineering Science, kanagawat@aees.kyushu-u.ac.jp
†Assistant professor, Department of Advanced Energy Engineering Science, yamamoto@aees.kyushu-u.ac.jp
‡ Assistant professor, Department of Advanced Energy Engineering Science,kajimura@aees.kyushu-u.ac.jp
¶ Professor, Department of Advanced Energy Engineering Science, nakasima@aees.kyushu-u.ac.jp
§ Postdoctoral fellow, Department of Electrical Engineering, masui@ele.kyutech.ac.jp

I. Introduction

The adoption of small satellites, with their flexibility, short development time and low cost, has been a breakthrough in space application. Therefore, small satellites have been researched and developed at several laboratories.[1,2]

An ion engine produces high thrust efficiency, exceeding 70%, with specific impulse of 3,000-8,000 s. Therefore, miniature ion engines are candidates for use as miniature propulsion system for small satellites.[3] The adoption of ion engines for small satellites will lead to the expansion of satellite's capability. That is, missions such as Mars exploration and self-disposal of satellites would be possible.[4]

A microwave discharge ion thruster is one of the ion thrusters. It will have longer lifetime and higher reliability compared to conventional electron bombardment-type ion engine, since there are no failures caused by cathodes degradation.[5]

Therefore, a 30 W class miniature ion thruster has been developed for de-orbiting 100 kg class satellites.[6] For easy ignition, high plasma density, with small space and low input power, an electrode microwave discharge ion source is used. The thrust performance of the miniature microwave discharge ion thruster has thus far been inferior to conventional ion thrusters, however, due to the high cost of ion production due to poor microwave-plasma coupling as well as high losses from ion and electron collisions with the walls. This type of ion source has a magnetic tube formed by a magnetic circuit and an antenna to emit microwaves. The magnetic tube would works as a virtual cathode, since the trapped electrons would gain energy from the microwaves by electron cyclotrons resonance (ECR) heating and would ionize neutral atoms. Therefore, thruster configurations, antenna configuration and magnetic field configuration, would affect the thrust performance.[7]

Hence, investigating the dependency of the internal plasma structure in the thruster is essential on magnetic field configuration for developing the miniature microwave discharge ion thruster. It is, however, difficult to measure inner properties of the plasma, since the ion engine is so small that we cannot insert a measurement equipment without perturbations. Numerical simulations are effective tool to understand the phenomena occurring in a miniature microwave ion thruster. So far, several studies have been conducted on numerical simulation of microwave ion source, [8] however no report was made on numerical simulation for a miniature microwave ion thruster.

We have developed a code coupling particle-in-cell (PIC) method and finite difference time domain (FDTD) one.[9] Adopting these methods has advantages in that PIC method can treat collision process and distribution function while FDTD method can analyze absorption of microwave in plasma. Analysis of the microwave ion thruster by using this code will also be very useful for developing microwave plasma sources employing antennas.[10]

In this study, we investigate the effects of magnetic field configuration on the thrust performance of the miniature microwave discharge ion thruster. The mechanism of energy transfer from the microwave to the electron and the distribution of electron energy are investigated with the numerical code.

II. Calculation Method

A. PIC Method

For the analysis of plasma behavior in the discharge chamber, the PIC method is used. Effects of electromagnetic field on plasma particles are calculated by linear interpolation in the PIC method. Fundamental equation for the method is the motion equation for electrons given as follows.

$$m\frac{d\boldsymbol{v}}{dt} = q\left(\boldsymbol{E} + \boldsymbol{v}\times\boldsymbol{B}\right) \tag{1}$$

Integration with respect to time is conducted by leap-flog method. In the PIC method, the electron-neutral collisions such as elastic, excitation and ionization processes are included and they are treated by Monte Carlo method and Null-collision method.[11] Among these collision processes, electron's energy losses are different. The present calculation treats xenon as the neutral particle. Cross section data used in the code are taken from Ref.12.

B. FDTD Method

Microwave propagation is analyzed by using FDTD method. Fundamental equation for the method is Maxwell's equation given as follows.

$$\nabla \times \boldsymbol{E} = -\mu_0 \frac{\partial \boldsymbol{H}}{\partial t} \tag{2}$$

$$\nabla \times \boldsymbol{H} = \varepsilon_0 \frac{\partial \boldsymbol{E}}{\partial t} + \boldsymbol{J} \tag{3}$$

Electromagnetic field components are defined at specific points of unit cells as suggested by Yee.[13] This arrangement permits a natural satisfaction of rotation with respect to space.

In the coupling code, time evolution is solved by exchanging the electric field and current density between PIC method and FDTD one.[14] Figure 1 shows a flow chart of the code. The calculation coordinate system used here is three-dimensional. The code has the capability to include three-dimensional structure such as L shaped antenna.

We here focus on the interaction among electron, microwave and magnetic field configuration. Only electron motion is taken into account of the calculation, that is, electrons gain its energy from the microwaves and ionizes neutral particles. Plasma production by the ECR heating is dominated by electron's behaviors, and ions are treated as background. In the coupling code, the static electric field induced by the charge separation between electrons and ions is not considered and then the Poisson equation is not solved. Thus, it is required to simulate the sheath on the boundaries of the conductor and magnet.

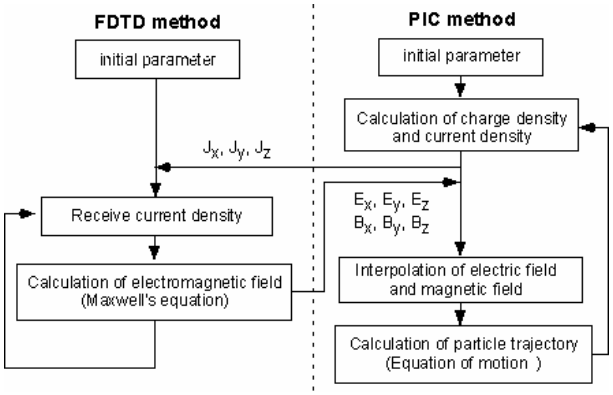

Figure 1. Coupling code flow chart.

C. Boundary Condition

We introduce the sheath model[15] given as follows. For electrons reaching the boundary, an electron having the energy less than 20 eV is reflected on the surface boundary, and an electron having larger than 20 eV is removed from the calculation region. The collision between an antenna and an electron is not considered. For the boundary condition of the microwaves, a perfect reflection condition is adopted on a yoke and a perfect conductor. Mur's first absorption boundary condition is adopted in the absorption boundary. [16]

D. Calculation Geometry and Parameter

The cross section of the miniature microwave discharge ion engine is shown in Fig.2. The calculation geometry is made for the Cartesian coordinate system and one cell is a cube of 0.5 mm in length. A magnetic circuit consists of some Sm-Co permanent magnets and iron yokes. The magnetic field intensity is varied by changing the number of magnets, N_{mag}. The calculated results are shown in Fig.3. With increase in the number of magnets, the location of ECR layer has moved.

The calculation conditions are given in Table 1. Time steps are different between PIC method and FDTD one. Since the stability conditions are different between those methods, and the time step in PIC method is increased for decreasing its calculation load.

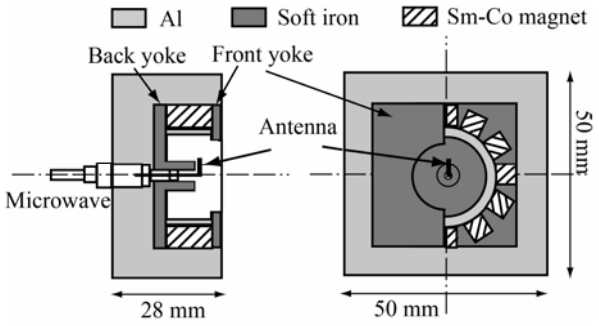

Figure 2. Cross section of miniature microwave discharge ion engine developed at Kyushu University.

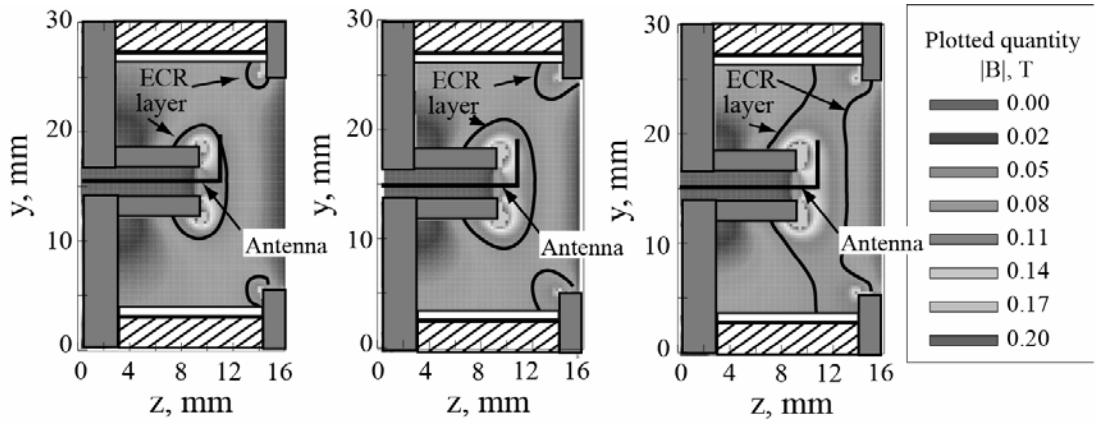

Figure 3. Magnetic field profile for each N_{mag}.
(a) N_{mag} = 9, (b) N_{mag} = 10, (c) N_{mag} = 11.

Table 1 .Calculation Parameter.

Time step (FDTD)	5.0×10^{-13} s
Time step (PIC)	1.0×10^{-12} s
Mesh size	5.0×10^{-4} m
Microwave frequency	2.45 GHz
Propellant	Xenon
Initial plasma density	1.0×10^{17} m^{-3}
Input power	8 W

III. Results and Discussion

A. Electron Trajectory

Figure 4 shows electron trajectories at N_{mag}=9, 10, and 11. As shown in Fig.4 (a), the electron at its initial position moves toward front yoke side, and then it is reflected in the vicinity of the front yoke. Then it moves toward the back yoke. The electron crosses the ECR layer and it is then reflected again nearby back yoke. As shown in Fig.4 (b) and Fig.4 (c), the respective electron bounces between the front yoke and the back yoke as in Fig.4 (a). It was confirmed that in this way electrons bounce between the magnetic mirrors.

Figure 5 shows the time variations of E_e and B_e at N_{mag}=9, 10, and 11. Here, E_e and B_e are electron energy and the magnetic field which the electron feels. Considering the relation between E_e and B_e for the electron behavior in Fig.5 (a), we can see that the electron gains energy when the electron crosses the ECR layer in the vicinity of the antenna. But the electron scarcely obtains energy when the electron crosses the ECR layer which locates far from the antenna. From Fig.5 (b), it is found that when the electron crosses the ECR which locates near the antenna, it is not heated effectively. This may be because the electric field component which is perpendicular to the magnetic field is not high there. In order to increase the electron energy efficiently, a high value of the component is necessary.[17] From Fig.5 (c), the electron scarcely obtains energy because it does not cross the ECR layer.

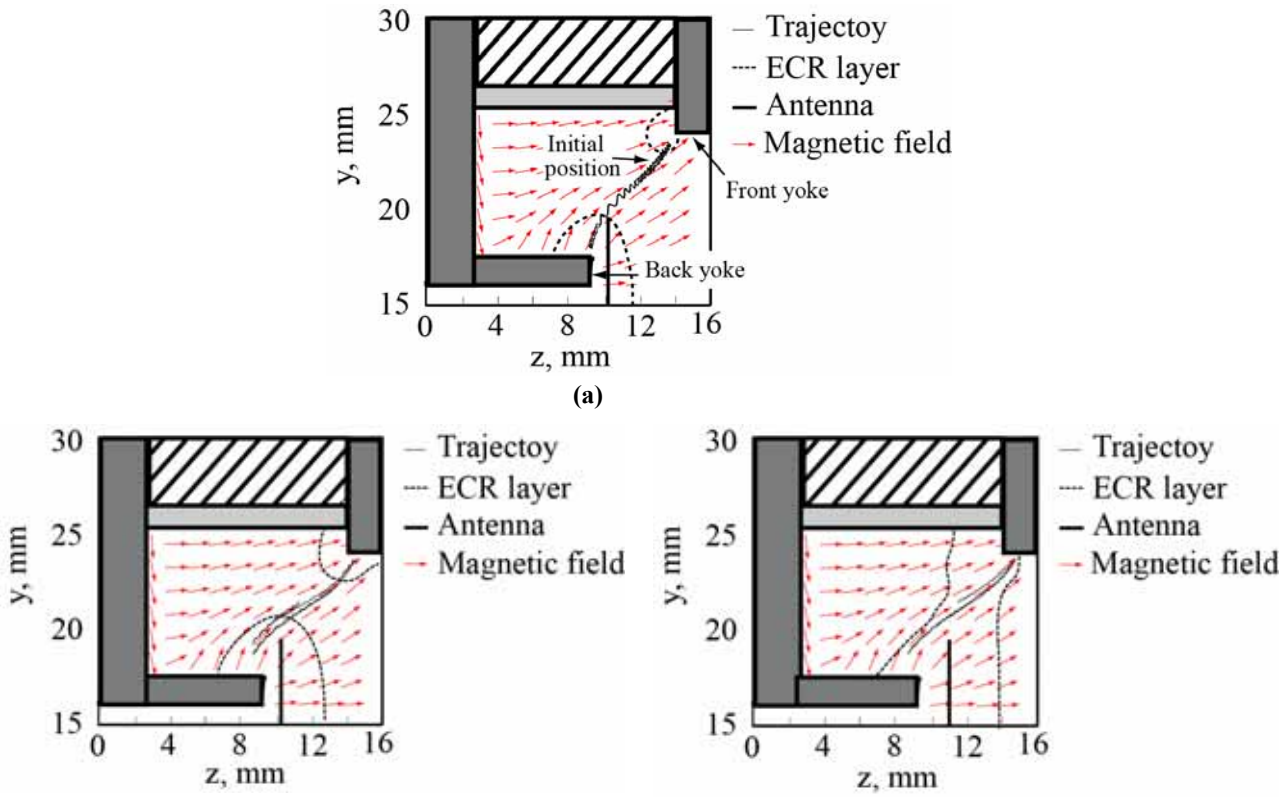

(a) **(b)** **(c)**

Figure 4. Electron trajectory.
(a) N_{mag} = 9, (b) N_{mag} = 10, (c) N_{mag} = 11.

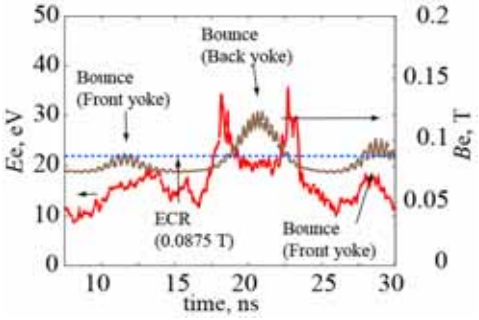

(a)

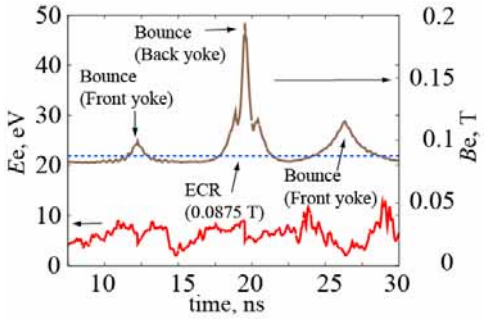

(b)

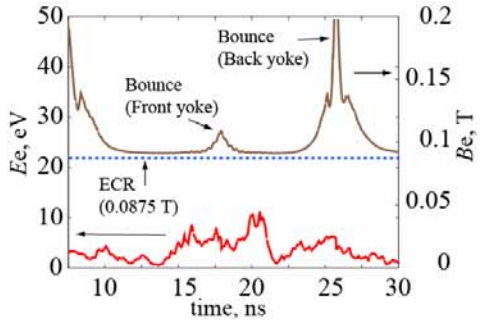

(c)

Figure 5. Time variations of E_e and B_e.
(a) N_{mag} = 9, (b) N_{mag} = 10, (c) N_{mag} = 11

B. Energy Variations ΔE after an Electron Crosses the ECR Layer

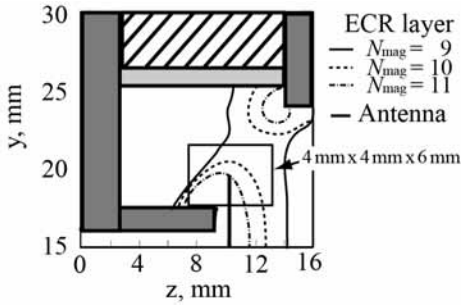

Figure 6. Calculated area.

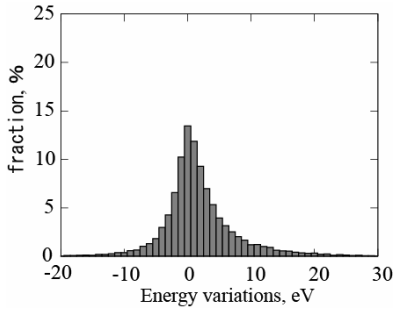

(a)

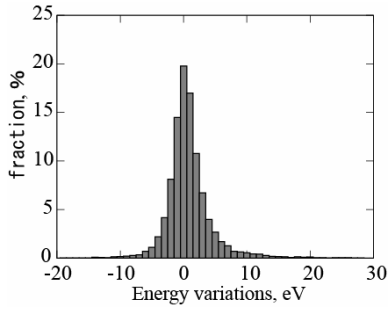

(b)

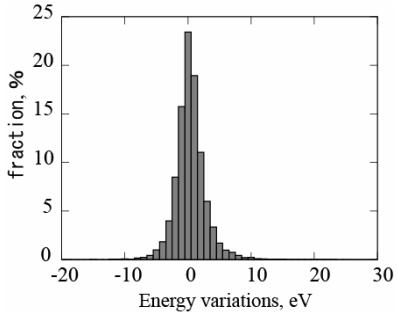

(c)

Figure 7. Distribution of Energy variations ΔE.
(a) N_{mag}=9, (b) N_{mag}=10, (c) N_{mag}=11.

ΔE after passing through the ECR layer in the vicinity of the antenna was calculated. The calculated area is shown in Fig.6. Figure 7 shows the distributions of ΔE at N_{mag}=9, 10, and 11. As shown in Fig.7, the fraction of electrons with high energy gain is decreased with increase in the number of magnet. The average values of gain energy for N_{mag}=9, 10, and 11 are 3.8 eV, 2.4 eV and 1.9 eV, respectively. These results show that electrons must be confined by the magnetic mirror and bounce in the magnetic tube many times in order to gain an energy larger than the ionization potential (12.13 eV) of xenon, though there are a few electrons which gain an energy higher than the potential after passing through the ECR once.

Therefore, the sheath potential adopted is important, since electrons are reflected in the vicinity of the front yoke and the back yoke, and there are a lot of electrons reflected by the sheath potential. In this study, we assumed that the sheath potential is 20 eV as the boundary condition. But it is necessary to consider a self-consistent sheath model in order to simulate the internal mechanism in the ion thruster more correctly.

C. Spatial Distribution of Electron Energy

A spatial distribution of electron energy E_e at 50 ns is shown in Fig.8. As shown there, the zone of high electron energy is decreased with increase in the number of magnet. Because electrons heated by the antenna move to the front yoke side through magnetic tube, the high energy region is larger at N_{mag} = 9. Moreover, the shape of the high energy zone is formed along the magnetic tube since the high energy electrons are trapped in the magnetic tube. These results show that magnetic tube works as the virtual cathode, that is, the trapped electrons by the magnetic tube gain energy from the microwaves by electron cyclotrons resonance (ECR) heating and ionize neutral atoms. On the other hand, the zone of high energy electron does not diffuse from the antenna to the grid, though the distance of the ECR layer and the antenna is close. This is due to electron collisions with the grid at z=16 mm. Because the magnetic mirror is not formed near the grid by the magnets, electrons are not reflected there.

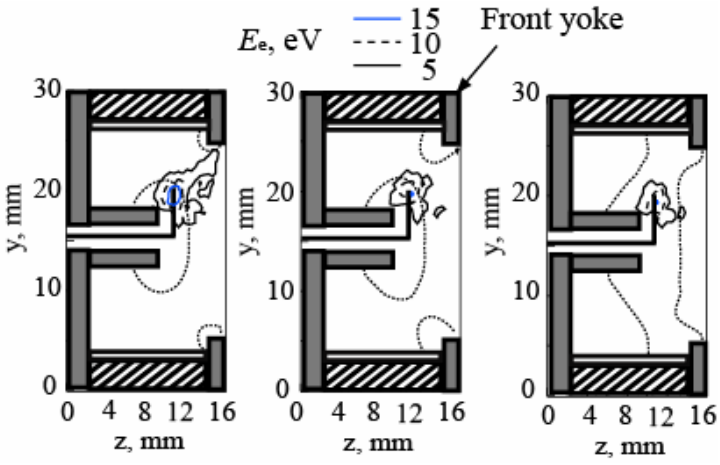

Figure 8. Spatial distribution of electron energy. (a) N_{mag} = 9, (b) N_{mag} = 10, (c) N_{mag} = 11.

C. Electron Energy Distribution Function (EEDF)

This section describes a comparison of EEDF among the three cases. In this calculation, EEDF is obtained in the area shown in Fig.9 and the calculated results are shown in Fig.10. The value of 12.13 eV is the ionization energy for xenon. The number of electrons having energies larger than the ionization energy is largest for N_{mag}=9.

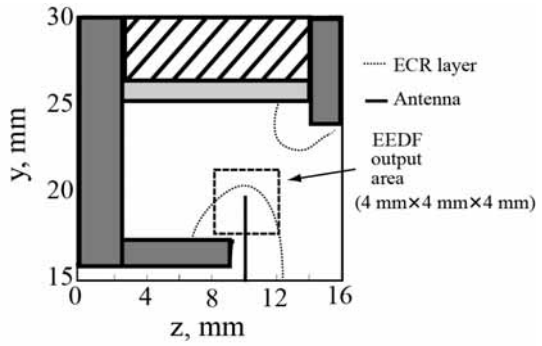

Figure 9. EEDF output area.

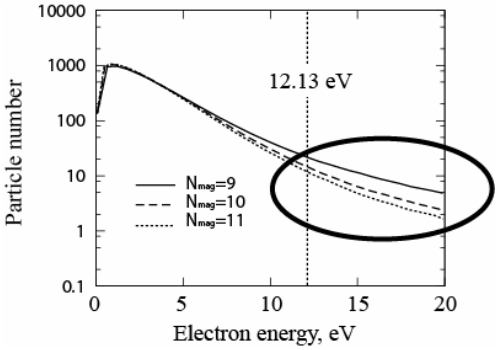

Figure 10. EEDF.

IV. CONCLUSION

The effect of magnetic field configuration on thrust performance in the miniature microwave discharge ion thruster was investigated with numerical simulation. The results obtained are as follows.

1) The electron trajectories were examined at N_{mag}=9, 10, and 11. It was confirmed that electrons bounce between the magnetic mirrors. Increasing the number of magnets, the trajectory was not so changed. But the time variation of electron energy is different whether the ECR layer is in a vicinity of the antenna, or not. In order to increase the electron energy efficiently, it is necessary to put an antenna in the vicinity of the ECR layer.
2) Energy variations after an electron crosses the ECR layer in the vicinity of the antenna were examined. 6.1 percent of the electrons for N_{mag}=9 obtain the energy above 12 eV after passing through the ECR layer once. It means that the electron which is shown in Fig. 5 (a) is not special. It is not necessary to bounce between the magnetic mirrors for these electrons. However, the averages of energy gain for N_{mag}=9, 10, and 11 are 3.8 eV, 2.4 eV and 1.9 eV, respectively. Most electrons must cross the ECR layer many times to gain an energy higher the ionization energy. Thus, it is necessary to consider the change of sheath potential with magnetic field strength change.
3) Energies of many electrons were examined by calculating spatial distributions of electron energy and electron energy distribution function. The zone of high electron energy and the number of electrons having energies larger than the ionization energy are decreased with increase in the number of magnet. This is because the distance between the ECR layer and antenna becomes longer. In the experiment, it is found that the increase in the distance between the ECR layer and antenna causes the poor microwave-plasma coupling .[18]

Acknowledgments

The present work was supported by a Grant-in-Aid for Scientific Research (C) (2), No. 16560691, and a Grant-in-Aid for Young Scientists (B), No. 17760638, sponsored by the Japan Society for the Promotion of Science, Japan.

Rerernces

[1]M. Kato, S. Takayama, U. Nakamura, K. Yoshihara and H. Hashimoto, Congress paper IAC-05.B5.6.B.01, 2005
[2]H. Sahara, S. Nakasuka and C.Kobayashi, AIAA paper 2005-3956, 2005.
[3]J. Muller, C. Marrese, J. Polk, E. Yang, A. Green, V. White, D. Bame, I. Chadraborty and S. Vargo, *Acta Astronautica*, Vol.52, 2003, pp.881-895.
[4]P. J. Wilbur, V. K. Rawlin, and J. R. Beattie, *J. of Propulsion and Powe*r, Vol.14, 1998, pp.708-715.
[5]H. Kuninaka and S. Satori, *Journal of Propulsion and Power*, Vol.14, 1998, pp.1022-1026.
[6]N.Yamamoto, H. Kataharada, H. Masui, H. Ijiri, and H. Nakashima, AJCPP2005-22093, 2005.
[7]N.Yamamoto, H. Kataharada, T. Chikaoka, H. Masui, and H.Nakashima,IEPC-2005-036, 2005.
[8]M. Hirakawa and M. Nakakita, Trans. Japan Aero. Space Sci. Vol.47, 1999, pp.267-271, (in Japanese).
[9]H. Masui, T. Tanoue, H. Nakashima and I. Funaki, 24th International Symposium on Space Technology and Science, paper ISTS 2004-b-11, 2004.
[10]Y. Takao, H. Masui, T. Miyamoto, H. Kataharada, H. Ijiri and H. Nakashima, Vacuum, Vol.73, 2004, pp.449-454.
[11]C. B. Opal, W. K. Peterson and E. C. Beaty, The Journal of Chemical Physics, Vol.55 ,1971, pp.4100-4106.
[12] J. J. Szabo, Jr., M. Martinez-Sanchez and O. Batishchev, AIAA paper 00-3653, 2000.
[13]K. S Yee, IEEE Trans. Antennas Propagat., Vol.14,1966, pp.302-307.
[14]V. P. Gropinath and T. A. Grotjohn, IEEE Trans. Plasma Sci,Vol. 23,1995,pp.602-608.
[15]J. C. Adam, A. Heron and G. Label, Phys. Plasmas, Vol.11, 2004,pp.295-305.
[16]G. Mur, IEEE Trans. Electromagn. Compat.Vol.23,1981,pp.377-382.
[17]H. Masui, Ph D. Diss., The Univ. of Kyushu, Department of Aeronautics and Astronautics, 2006 (in Japanese).
[18]T. Chikaoka, S. Kondo, N. Yamamoto, H. Nakashima and Y. Takao, Proceedings of the 25th International Symposium on Space Technology and Science, 2006, pp.254-259.